Received: 4 August 2022 | Revised: 5 January 2023 | Accepted: 11 January 2023

DOI: 10.1111/mpp.13300

Molecular Plant Pathology WILEY

ORIGINAL ARTICLE

Suppression of citrus canker disease mediated by flagellin perception

Maxuel de Oliveira Andrade | Jaqueline Cristina da Silva | Adriana Santos Soprano | Hugo Massayoshi Shimo | Adriana Franco Paes Leme | Celso Eduardo Benedetti

Brazilian Biosciences National Laboratory (LNBio), Brazilian Center for Research in Energy and Materials (CNPEM), Campinas, Brazil

Correspondence
Celso Eduardo Benedetti and Maxuel de Oliveira Andrade, Brazilian Biosciences National Laboratory (LNBio), Brazilian Center for Research in Energy and Materials (CNPEM), CEP 13083-100, Campinas, SP, Brazil.
Email: celso.benedetti@lnbio.cnpem.br; maxuel.andrade@lnbr.cnpem.br

Funding information
Conselho Nacional de Desenvolvimento Científico e Tecnológico, Grant/Award Number: 303238/2016-0 and 164832/2017-3; Fundação de Amparo à Pesquisa do Estado de São Paulo, Grant/Award Number: 2020/02547-0, 2018/08535-4 and 2014/50880-0

Abstract

Citrus cancer, caused by strains of *Xanthomonas citri* (Xc) and *Xanthomonas aurantifolii* (Xa), is one of the most economically important citrus diseases. Although our understanding of the molecular mechanisms underlying citrus canker development has advanced remarkably in recent years, exactly how citrus plants fight against these pathogens remains largely unclear. Using a Xa pathotype C strain that infects Mexican lime only and sweet oranges as a pathosystem to study the immune response triggered by this bacterium in these hosts, we herein report that the Xa flagellin C protein (*XaFliC*) acts as a potent defence elicitor in sweet oranges. Just as Xa blocked canker formation when coinfiltrated with Xc in sweet orange leaves, two polymorphic *XaFliC* peptides designated flgIII-20 and flgIII-27, not related to flg22 or flgII-28 but found in many *Xanthomonas* species, were sufficient to protect sweet orange plants from Xc infection. Accordingly, ectopic expression of *XaFliC* in a Xc *FliC*-defective mutant completely abolished the ability of this mutant to grow and cause canker in sweet orange but not Mexican lime plants. Because *XaFliC* and flgIII-27 also specifically induced the expression of several defence-related genes, our data suggest that *XaFliC* acts as a main immune response determinant in sweet orange plants.

KEYWORDS
Citrus sinensis, citrus canker, *Xanthomonas citri*, *Xanthomonas aurantifolii* pathotype C, flagellin C, flgIII-20, flgIII-27, *FliC*

1 | INTRODUCTION

Citrus canker, caused by the bacterial pathogen *Xanthomonas citri* (Xc), also referred to as *X. citri* pv. *citri*, is one of the most important citrus diseases and affects all commercial citrus varieties causing great economic losses to the citrus industry worldwide. The disease is characterized by water-soaked and eruptive lesions that develop on leaves, fruits, and twigs, causing defoliation, premature fruit drop, and general tree decline (Brunings & Gabriel, 2003; Graham et al., 2004).

Different strains of Xc have been isolated from numerous citrus hosts around the world. The Xc Asiatic or type A strains are widely spread in citrus-producing areas, cause the most severe canker symptoms, and have a broad host range, infecting all commercial orange (*Citrus sinensis*), lemon (*Citrus limon*), grapefruit (*Citrus paradisi*), and mandarin orange (*Citrus reticulata*) varieties. On the other hand,

Maxuel de Oliveira Andrade and Jaqueline Cristina da Silva contributed equally to this work.

the related canker pathogen *Xanthomonas aurantifolii* (Xa), also classified as *X. citri* pv. *aurantifolii*, *Xanthomonas fuscans* pv. *aurantifolii*, or *X. citri* pv. *fuscans*, causes cankers on a limited number of citrus plants and is restricted to certain regions of Brazil and Argentina (Brunings & Gabriel, 2003). In particular, the Xa pathotype C strain ICMP 8435, henceforth called Xa, causes typical canker symptoms on Mexican lime (*Citrus aurantifolia*) trees only, whereas in sweet oranges it triggers a basal defence response that halts canker development (Cernadas et al., 2008).

The precise molecular mechanisms by which Xc induces cell growth and division in citrus, the hallmarks of canker lesions, are not fully understood. However, numerous studies carried out in the last two decades revealed that transcriptional activator-like (TAL) effectors of the AvrBs3/PthA family play an essential role in triggering the transcriptional reprogramming of citrus cells, leading to cell hypertrophy and hyperplasia, the main host physiological and morphological changes that favour pathogen growth and spread. Of note, *PthA4*, the only Xc *PthA* variant that is essential for full canker symptom development, directly transactivates the citrus *LOB1* gene (*CsLOB1*), which appears to function as a master regulator of downstream genes that control cell division and expansion (Abe & Benedetti, 2016; Al-Saadi et al., 2007; Brunings & Gabriel, 2003; Duan et al., 2018; Hu et al., 2014; Pereira et al., 2014). Moreover, *PthA4* has also been shown to interact with host proteins implicated in transcriptional control, including CsMAF1, a cell growth regulator and negative modulator of RNA polymerase III (Oliveira Andrade et al., 2020; Soprano et al., 2013, 2017; de Souza et al., 2012).

On the other hand, it remains largely unknown how citrus plants fight against Xc infection and what are the main molecular determinants underlying the immune response triggered by Xa in sweet orange plants. Although *PthA* variants from Xc strains have recently been shown to trigger immune responses on certain citrus hosts (Roeschlin et al., 2019; Teper et al., 2021), none of the *PthA*-related effectors of Xa B and C strains, referred to as *PthB* and *PthC*, appear to act as avirulence factors on citrus (Al-Saadi et al., 2007; Brunings & Gabriel, 2003). Accordingly, the ectopic expression of a Xa PthC effector in sweet orange epicotyls did not obviously induce the expression of defence executor genes (Pereira et al., 2014), which is also consistent with the fact that the *pthC* knockout mutant of a Xa C strain lost its pathogenicity in Mexican lime but not the ability to trigger a hypersensitive response (HR) in grapefruit (Al-Saadi et al., 2007). These results thus suggest that, at least for Xa C isolates, TAL effectors do not seem to play a critical role in the immune response triggered by this bacterium in sweet orange and grapefruit. Moreover, the observation that *X. citri* pv. *aurantifolii* B and C strains have a reduced repertoire of pathogenicity-related genes, which in principle could explain the narrower host range and lower aggressiveness of these pathogens compared to Xc strains (Fonseca et al., 2019), offers no clues as to the mechanism by which Xa triggers an immune response in sweet oranges. In line with this idea, it was shown that a *X. fuscans* pv. *aurantifolii* C strain, which causes canker only in key lime (*C. aurantifolia*), possesses a type III effector of the XopAG family, named *AvrGf2*, that is responsible for the HR observed in grapefruit (Gochez et al., 2015). *AvrGf2* interacts with grapefruit cyclophilin GfCyp (Gochez et al., 2017); nevertheless, the precise mechanism by which *AvrGf2* triggers an HR in grapefruit remains unclear.

Large-scale transcriptional analyses of sweet orange plants challenged with Xa, relative to Xc, revealed that, in contrast to Xc, Xa strongly up-regulates a set of defence-related genes very early during infection, encoding, for instance, the mitogen-activated protein kinase CsMAPK1, several WRKY factors, and pathogenesis-related (PR) proteins, consistent with pathogen-associated molecular pattern (PAMP)-induced activation of a defence MAPK signalling cascade (Cernadas et al., 2008; de Oliveira et al., 2013). In fact, the augmented expression of CsMAPK1 in transgenic Troyer citrange plants was correlated with a decrease in Xc growth in infected leaves, accompanied by an increase in PR gene expression and reactive oxygen species (ROS) production and a reduction in canker pustule formation (de Oliveira et al., 2013). Thus, the characteristics of the immune response observed in sweet orange plants in response to Xa infection are consistent with a PAMP-triggered immunity (PTI) type of defence response. Although plants recognize a wide range of bacterial PAMPs, flagellin has been reported as one of the major innate immunity elicitors in many plant–bacterial interactions (Cai et al., 2011; Clarke et al., 2013; Gomez-Gomez & Boller, 2002; Nicaise et al., 2009; Wang et al., 2015; Zipfel et al., 2004). Because we found variations in the amino acid sequence between the flagellin C (*FliC*) proteins isolated from Xc (*XcFliC*) and Xa (*XaFliC*) and because *FliC* polymorphism has been reported to affect elicitation as well as evasion of plant defences (Malvino et al., 2022; Sun et al., 2006; Wei et al., 2020), we decided to investigate whether *XaFliC* could be involved in the immune response triggered by Xa in sweet orange plants.

Here, we present evidence that *XaFliC* is sufficient to trigger a robust defence response that completely halts the development of canker lesions caused by virulent Xc in sweet oranges but not Mexican lime plants. We also show that two polymorphic peptides of *XaFliC*, denoted here as flgIII-20 and flgIII-27, which are not related to the well-known flg22 and flgII-28 peptides, also protected sweet orange leaves from Xc infection. To the best of our knowledge, this is the first description of *FliC* as a PAMP or molecular determinant of an immune response induced by a citrus canker pathogen.

2 | RESULTS

2.1 | Xa protects sweet orange leaves from Xc infection

It is well established that Xa triggers a basal defence response in all commercial sweet orange varieties (Brunings & Gabriel, 2003; Cernadas et al., 2008). To verify whether this defence response could prevent Xc infection and canker formation, sweet orange leaves of cultivars Natal and Pera were infiltrated with a mixed suspension of Xa and Xc cells at a 1:1 ratio. In comparison to leaf sectors inoculated

with Xa or Xc alone at equivalent cell densities, used as controls for the basal defence response and canker development, respectively, leaf sectors infiltrated with the mixed Xa + Xc suspension showed no canker symptoms, in both Natal and Pera plants (Figure 1a). When Xa was infiltrated 24 h prior to Xc inoculation, the defence response still prevailed and no canker symptoms developed in either Natal or Pera leaves (Figure 1b). However, when Xc was infiltrated 24 h prior to Xa inoculation, canker symptoms developed normally on both citrus hosts (Figure 1c). These results show that the defence response induced by Xa in sweet orange leaves can suppress canker formation if triggered early or before Xc suppresses basal defences and establishes an infection.

2.2 | Xa-induced protection against Xc infection is time-dependent

The results shown in Figure 1 suggest that Xa-induced protection of sweet orange leaves against Xc infection is time-dependent. To further evaluate this response and test whether spray inoculation of Xa could also protect plants from Xc infection, leaves of Natal plants were sprayed with a Xa suspension, and after different time intervals Xc was infiltrated into the leaves. We found that spray application of Xa prevented canker formation only when Xc was infiltrated 24 h after spraying, whereas no protection was observed when Xc was infiltrated 4 h or 5 days after Xa application (Figure 2). These results suggest that the defence response triggered by Xa has a short time frame of hours after bacterial spraying, which is consistent with previous transcriptome analysis of Pera leaves challenged with this pathogen (Cernadas et al., 2008). Moreover, Xa-induced protection appears to require bacterial penetration into the leaf mesophyll, as canker symptoms developed normally in leaves sprayed with Xa 4 h before Xc infection (Figure 2), but not in leaves coinfiltrated or previously infiltrated with Xa (Figure 1a,b).

2.3 | Amino acid polymorphisms between Xa and Xc *FliC* proteins

The observation that bacterial penetration into the leaf mesophyll was critical for Xa-induced protection against Xc infection suggested that FliC, a major innate immunity elicitor in many plant–bacterial interactions, might be involved in this process. To investigate this possibility, we compared the amino acid sequences of FliC from Xa

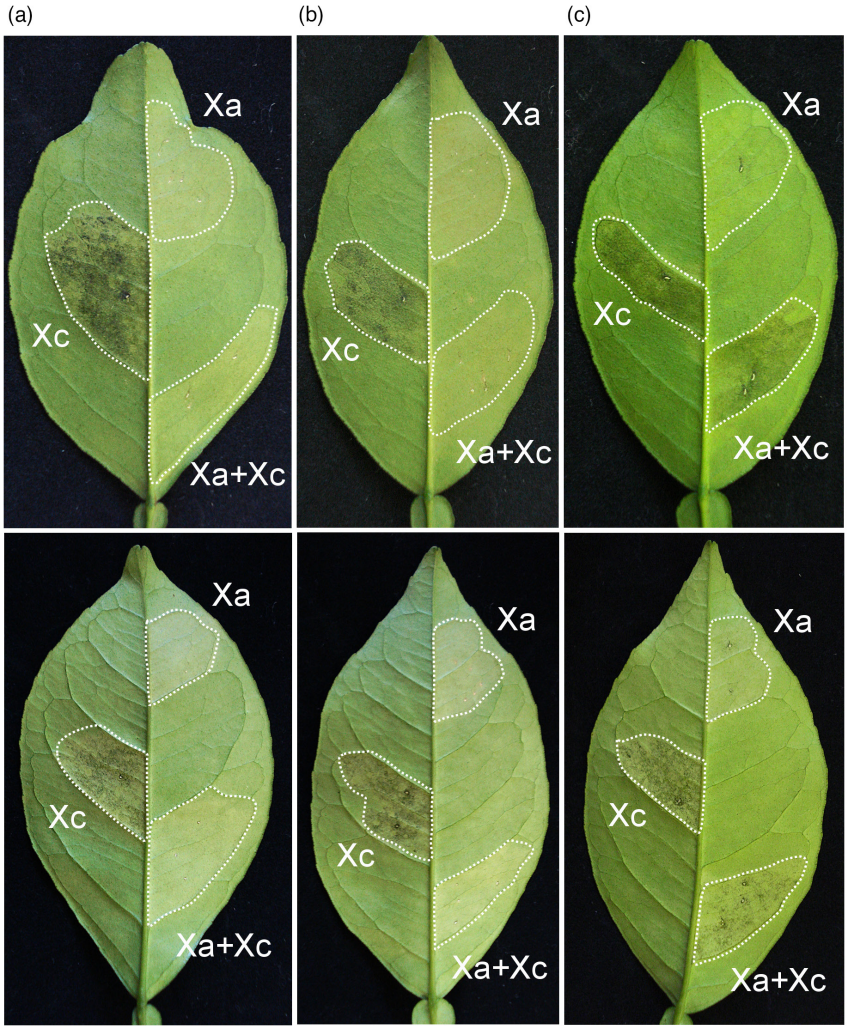

FIGURE 1 *Xanthomonas aurantifolii* (Xa) protects sweet orange leaves from *Xanthomonas citri* (Xc) infection. (a) Leaves of Natal (upper panel) and Pera (bottom panel) plants infiltrated with a suspension of Xc or Xa (OD_{600} = 0.1) or with a mixed suspension of Xa and Xc cells at a 1:1 ratio (Xa + Xc). Xa blocks canker development when simultaneously inoculated with Xc. (b) Twenty-four hours after Xa infiltration, Xc was inoculated in the same leaf area (Xa + Xc) and canker symptoms did not develop. (c) Twenty-four hours after Xc infiltration, Xa was inoculated in the same leaf area (Xa + Xc) and canker symptoms developed normally, indicating that Xc suppresses the Xa-triggered defence if established first. Infiltrated leaf sectors are indicated by the dashed lines and those inoculated with Xc or Xa separately served as controls. Canker symptoms were evaluated 10 days postinoculation. Three leaves of each citrus variety were infiltrated and the images presented are representative of the phenotype observed in all infiltrated leaves

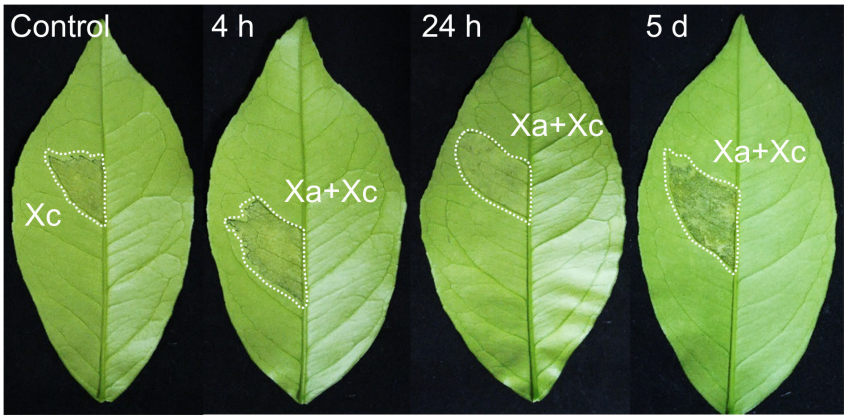

FIGURE 2 *Xanthomonas aurantifolii* (Xa)-induced protection against *Xanthomonas citri* (Xc) infection is time-dependent. Natal leaves were sprayed with a suspension of Xa (OD_{600} = 0.1) and after 4 h, 24 h, or 5 days, Xc (OD_{600} = 0.1) was infiltrated into the leaves (areas surrounded by dashed lines). Canker symptoms were recorded 10 days after Xc inoculation. Xa prevented canker formation when Xc was inoculated 24 h after Xa application. No protection was observed when Xc was inoculated 4 h or 5 days after the Xa treatment, indicating that the Xa-induced protection response has a short time frame of a few hours and requires bacterial penetration into the leaf mesophyll to occur. The images presented are representative of the phenotype observed in most infiltrated leaves

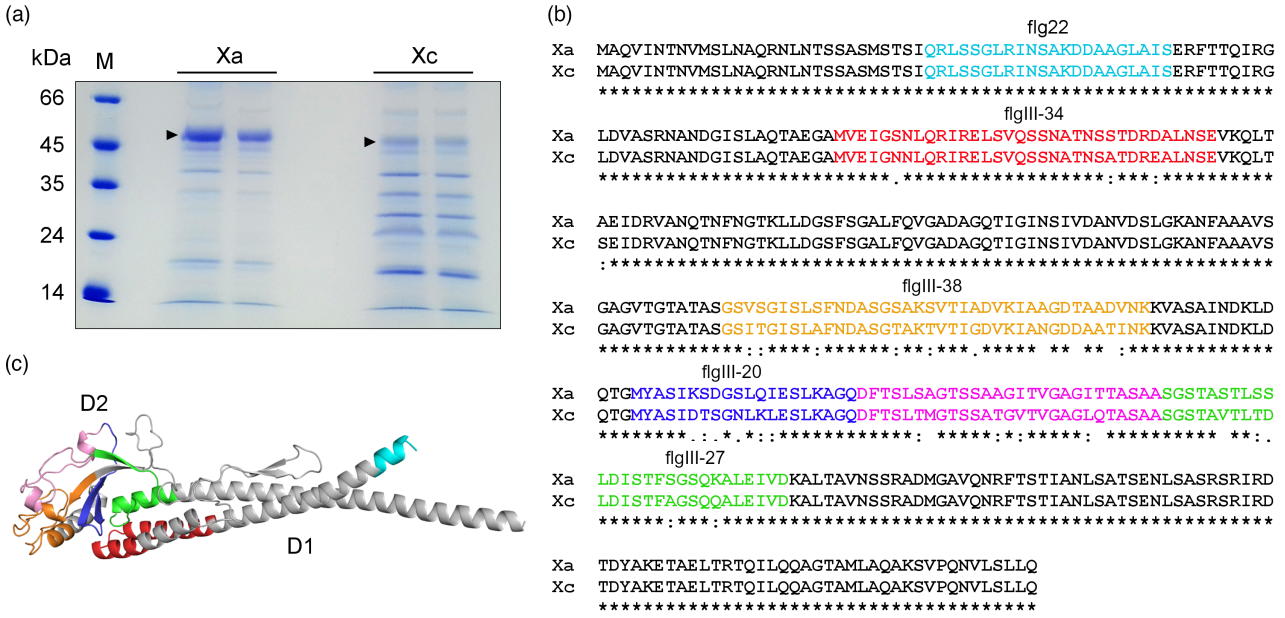

FIGURE 3 The *FliC* proteins from *Xanthomonas aurantifolii* (Xa) and *Xanthomonas citri* (Xc) display several amino acid polymorphisms. (a) SDS-PAGE of flagellum preparations showing the major approximately 50 kDa band corresponding to the *FliC* proteins from Xa and Xc (arrowheads). M indicates the molecular marker. (b) Protein sequence alignment performed with Clustal Omega showing that the amino acid polymorphisms between *XaFliC* (Xa) (GenBank accession WP_007962409) and *XcFliC* (Xc) (GenBank accession WP_003482972) lie outside of the flg22 region (coloured in cyan). Regions coloured in red (flgIII-34), orange (flgIII-38), blue (flgIII-20), magenta, and green (flgIII-27) represent the polymorphic peptides between the two *FliC* proteins. The flgIII-34 sequence includes the *Pseudomonas syringae* flgII-28 peptide. (c) Structural model of *XaFliC* based on the crystal structure of the *Sphingomonas* sp. A1 flagellin (PDB code 3K8V) showing that the corresponding polymorphic regions depicted in (b) are located mostly in the globular D2 domain

(*XaFliC*) and Xc (*XcFliC*). Because the genome of the Xa strain used in this study (ICMP 8435, Cernadas et al., 2008) is not available, flagella of Xa and Xc were extracted and proteins associated with this preparation were resolved by SDS-PAGE and identified by mass spectrometry (Figure 3). These analyses confirmed that the major approximately 50 kDa bands, observed at higher levels in Xa samples (Figure 3a), correspond to *FliC* proteins. All the peptides identified by mass spectrometry (Table S1) showed perfect matches to the *FliC* proteins of Xc and Xa strains deposited at the NCBI database with the reference sequences WP_003482972 and WP_007962409, respectively.

Protein sequence alignment revealed a number of amino acid polymorphisms between XaFliC and XcFliC (Figure 3b). Notably, all amino acid changes found between *XaFliC* and *XcFliC* lie outside the flg22 region (Figure 3b). Moreover, according to our structural models, most of the *FliC* polymorphic regions, hereinafter referred to as

the flgIII-20, flgIII-27, flgIII-34, and flgIII-38 peptides, are located in the *FliC* D2 domain (Figure 3b,c). The only exception is flgIII-34, which corresponds to the *Pseudomonas syringe* pv. *tomato* flgII-28, which is recognized by the tomato FLS3 receptor (Cai et al., 2011; Clarke et al., 2013) (Figure 3c).

2.4 | Polymorphic peptides from *XaFliC* protects citrus from Xc infection

The amino acid polymorphisms found between *XaFliC* and *XcFliC* suggested that a specific region of the *XaFliC* polypeptide could evoke the immune response triggered by Xa in sweet orange plants. To test this hypothesis, the five peptides spanning the *FliC* polymorphic regions (Figure 3b) were synthesized and coinfiltrated with Xc in Natal leaves. However, the peptide located between flgIII-20 and flgIII-27 (Figure 3b) was insoluble in aqueous solutions and thus could not be tested.

We found that while none of the *XcFliC* peptides affected canker development in sweet orange leaves, the *XaFliC* peptides flgIII-20 and flgIII-27 fully protected Natal leaves from Xc infection, as no canker symptoms developed in the leaf sectors coinfiltrated with them (Figure 4a). Similar results were observed in Troyer citrange leaves (Figure 4b). On the other hand, flgIII-20 and flgIII-27 derived from *XaFliC* only partially protected Mexican lime leaves from Xc infection (Figure 4c). Likewise, canker symptoms elicited by Xa in Mexican lime were slightly attenuated by the *XaFliC* flgIII-20 and flgIII-27 peptides (Figure 4d). Because all tested peptides did not inhibit Xc or Xa growth in culture medium (Figure S1), the results indicate that flgIII-20 and flgIII-27 derived from *XaFliC* elicit a robust defence response in Natal and Troyer, but not Mexican lime plants. In addition, to rule out the possibility that the flg22 peptide, which is

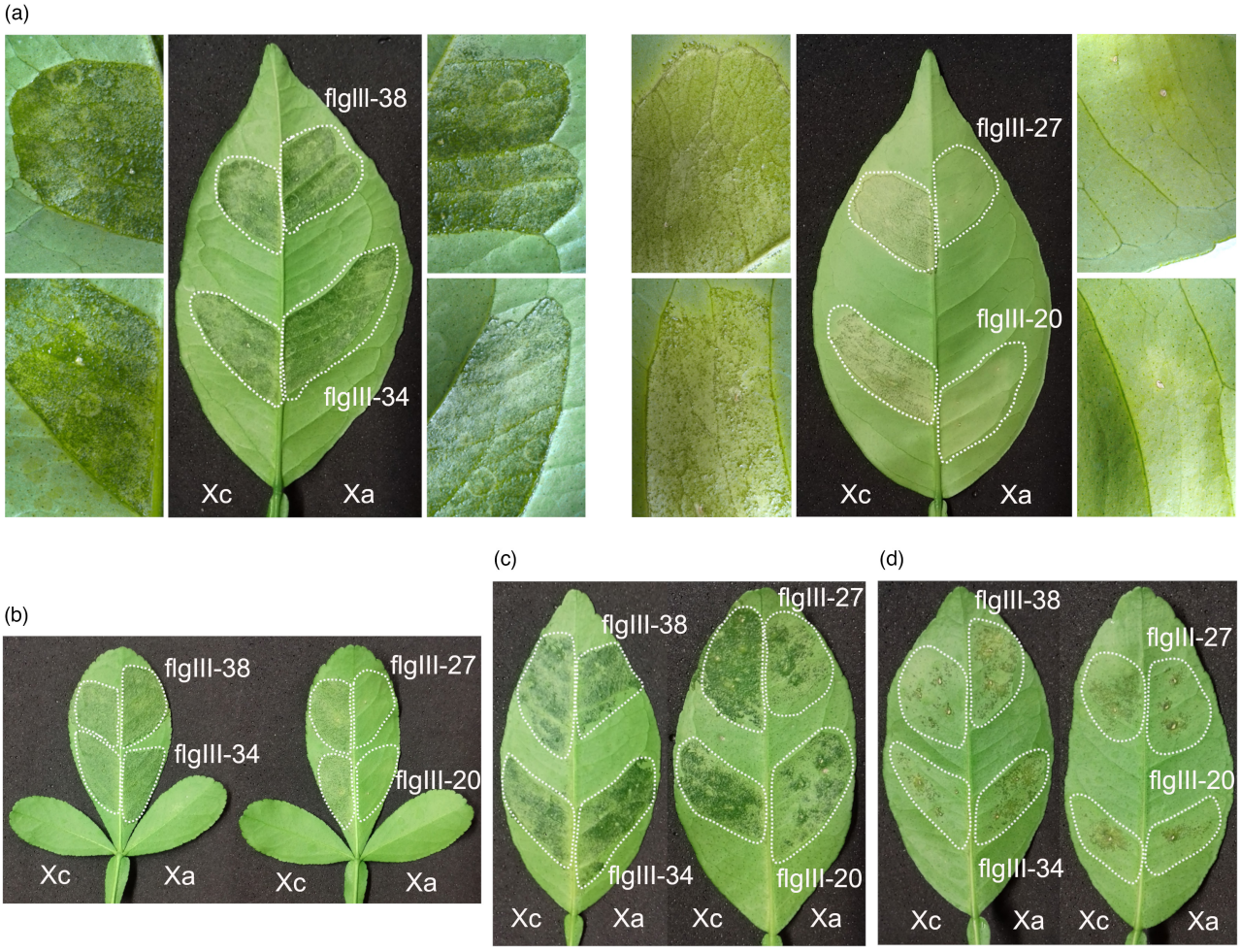

FIGURE 4 Polymorphic peptides from *XaFliC*, but not *XcFliC*, protected citrus from *Xanthomonas citri* (Xc) infection. (a) Natal leaves were infiltrated with a water suspension of Xc (OD_{600} = 0.05) in the presence of the *XcFliC* (Xc) or *XaFliC* (Xa) peptides at a final concentration of 70 μM (areas surrounded by dashed lines). Canker symptoms were recorded 10 days after bacterial inoculation. Only peptides flgIII-20 and flgIII-27 inhibited canker formation. Details of the infiltrated leaf sectors at higher magnification (10×) are shown on the left and right. (b) Same experiment performed with Troyer citrange showing that only peptides flgIII-20 and flgIII-27 protected leaves from Xc infection. (c) Peptides flgIII-20 and flgIII-27 partially protected Mexican lime leaves from Xc infection. (d) Peptides flgIII-20 and flgIII-27 attenuated canker development caused by *Xanthomonas aurantifolii* (Xa) in Mexican lime leaves. Three leaves of each citrus variety were infiltrated and the images presented are representative of the phenotype observed in most infiltrated leaves

identical between *XaFliC* and *XcFliC*, does not contribute to the defence response triggered by Xa in sweet oranges, Xc was infiltrated in the presence and absence of flg22 in Natal, Pera, and Valencia leaves. The results confirm that flg22 does not protect sweet orange leaves from Xc infection (Figure S2).

2.5 | *XaFliC* elicits canker resistance in sweet orange plants

To confirm the role of *XaFliC* as a major defence response elicitor in sweet orange plants, a Xa *fliC* mutant, defective in *XaFliC* production (XaΔ*fliC*), was generated and further complemented with the *XaFliC* gene, as revealed by western blot (Figure 5a) and cell motility assays (Figure 5b). We found that contrary to wild-type Xa, the XaΔ*fliC* mutant did not protect Natal, Pera, or Valencia leaves from Xc infection (Figure 5c). Although complementation of the XaΔ*fliC* mutant with *XaFliC* did not restore the protective role of Xa in most of the sweet orange varieties tested, except in Natal plants (Figure 5c), possibly due to low levels of complementation, as revealed by the motility assay (Figure 5b), the results do show that *XaFliC* contributes to the defence response triggered by Xa in sweet oranges. Interestingly, disruption of *XaFliC* was not sufficient to cause canker on sweet oranges (Figure S3); however, the reduction in leaf yellowing induced by the XaΔ*fliC* mutant, observed in Natal, Pera, and Sorocaba leaves (Figure S3), suggests that the *XafilC* mutation attenuated the defence response triggered by Xa in these hosts.

Next, we expressed the *XaFliC* gene in the Xc *FliC*-deletion mutant (XcΔ*fliC*). Western blot (Figure 5a) and bacterial motility assays (Figure 5b) confirmed that complementation of the XcΔ*fliC* mutant with the *XaFliC* gene not only restored but even increased bacterial motility, relative to wild-type Xc or the XcΔ*fliC* mutant transfected with empty vector, used as control (Figure 5b).

Plant inoculations with these bacterial mutants revealed that deletion of *FliC* in Xc did not alter canker development. Surprisingly, however, the expression of *XaFliC* in the XcΔ*fliC* mutant was sufficient to elicit a robust defence response in several sweet orange varieties, but not in Mexican lime, although canker symptoms produced by this mutant in Mexican lime were slightly reduced in comparison to wild-type Xc or XcΔ*fliC* transfected with empty vector (Figure 5d). In line with these results, bacterial counts on Natal leaves revealed that leaf sectors infiltrated with XcΔ*fliC* expressing *XaFliC* showed a marked reduction in bacterial growth at 3, 7, and 14 days after bacterial inoculation, compared to leaf sectors infiltrated with Xc or XcΔ*fliC* carrying the empty vector, used as control (Figure 5e). Conversely, the XcΔ*fliC* mutant expressing *XaFliC* reached much higher titres in Mexican lime leaves at 3 to 14 days postinoculation, although it grew more slowly than Xc or XcΔ*fliC* carrying the empty vector (Figure 5e), which is consistent with the fact that this mutant also induced less severe canker symptoms in lime relative to Xc or XcΔ*fliC* carrying the empty vector (Figure 5d).

Together, these results confirm that *XaFliC* is a major elicitor of the immune response triggered by Xa in sweet orange plants.

2.6 | *FLS2* and *WRKY22* induction in sweet orange is dependent on *XaFliC* expression

In a previous gene expression study using differential display and microarray analyses, we found that Xa induces the expression of several sweet orange genes involved in basal defence within 48 h of bacterial inoculation (Cernadas et al., 2008). To broaden our understanding of the transcriptional changes associated with the defence response triggered by Xa in sweet orange plants, we performed RNA sequencing (RNA-seq) analysis of Natal leaves infiltrated with Xa, Xc, or water, at 24 and 48 h after bacterial inoculation.

The RNA-seq data not only corroborated our previous gene expression studies (Cernadas et al., 2008; Pereira et al., 2014), but also revealed a larger number of innate immunity-related genes being predominantly or exclusively up-regulated by Xa, relative to Xc infection, including genes encoding several leucine-rich repeat–receptor-like kinases (RLKs), genes encoding transcription factors of the WRKY, BHLH, and MYB families, and genes associated with oxidative burst, the HR, and senescence (Data S1). Interestingly, while

FIGURE 5 *XaFliC* is the main elicitor of canker resistance in sweet oranges. (a) Western blot analysis showing the expression of *XaFliC* (arrow) in wild-type *Xanthomonas aurantifolii* (Xa) and *Xanthomonas citri* (Xc), *fliC* mutants XaΔ*fliC* and XcΔ*fliC*, and corresponding *fliC* mutants complemented with *XaFliC* (XaΔ*fliC*+*XaFliC*, XcΔ*fliC*+*XaFliC*). Blots were probed with anti-*XaFliC* serum. (b) Motility assays performed on soft agar showing that disruption or deletion of *FliC* in Xa and Xc significantly reduces bacterial motility. Complementation of these mutants with *XaFliC* only partially restored Xa motility, whereas in Xc, *XaFliC* expression significantly increased cell motility. (c) Leaves of Natal, Pera, and Valencia plants infiltrated with Xc (control) or with a mixed suspension ($OD_{600} = 0.1$) of Xc+Xa (Xa) or Xc+XaΔ*fliC* transformed with empty vector or vector expressing *XaFliC* (at a 1:1 ratio), showing that Xa but not XaΔ*fliC* blocks canker development when simultaneously inoculated with Xc. (d) Canker symptoms developed on Natal, Pera, Valencia, and Sorocaba sweet oranges and in Mexican lime leaves 10 days after they were infiltrated with a water suspension ($OD_{600} = 0.1$) of Xc or the corresponding XcΔ*fliC* mutants (areas surrounded by dashed lines). Expression of *XaFliC* in the XcΔ*fliC* mutant was sufficient to trigger a robust defence response in all sweet orange varieties tested, but not in Mexican lime. Three leaves of each citrus variety were infiltrated and the images presented are representative of the phenotype observed in most infiltrated leaves. (e) Bacterial counts on Natal and Mexican lime leaves infiltrated with wild-type Xc or XcΔ*fliC* transformed with *XaFliC* or the empty vector (EV), used as control, determined at 0, 3, 7, and 14 days post-infection (dpi). While in Natal leaves the XcΔ*fliC* mutant expressing *XaFliC* showed a sharp reduction in growth within 14 days of bacterial inoculation, relative to Xc or the XcΔ*fliC* mutant carrying the empty vector, this complemented strain reached much higher titres in Mexican lime leaves at 3, 7, and 14 dpi. Error bars represent standard deviations of three independent biological samples, and asterisks indicate statistically significant differences between the means at $\alpha = 0.05$ relative to Xc

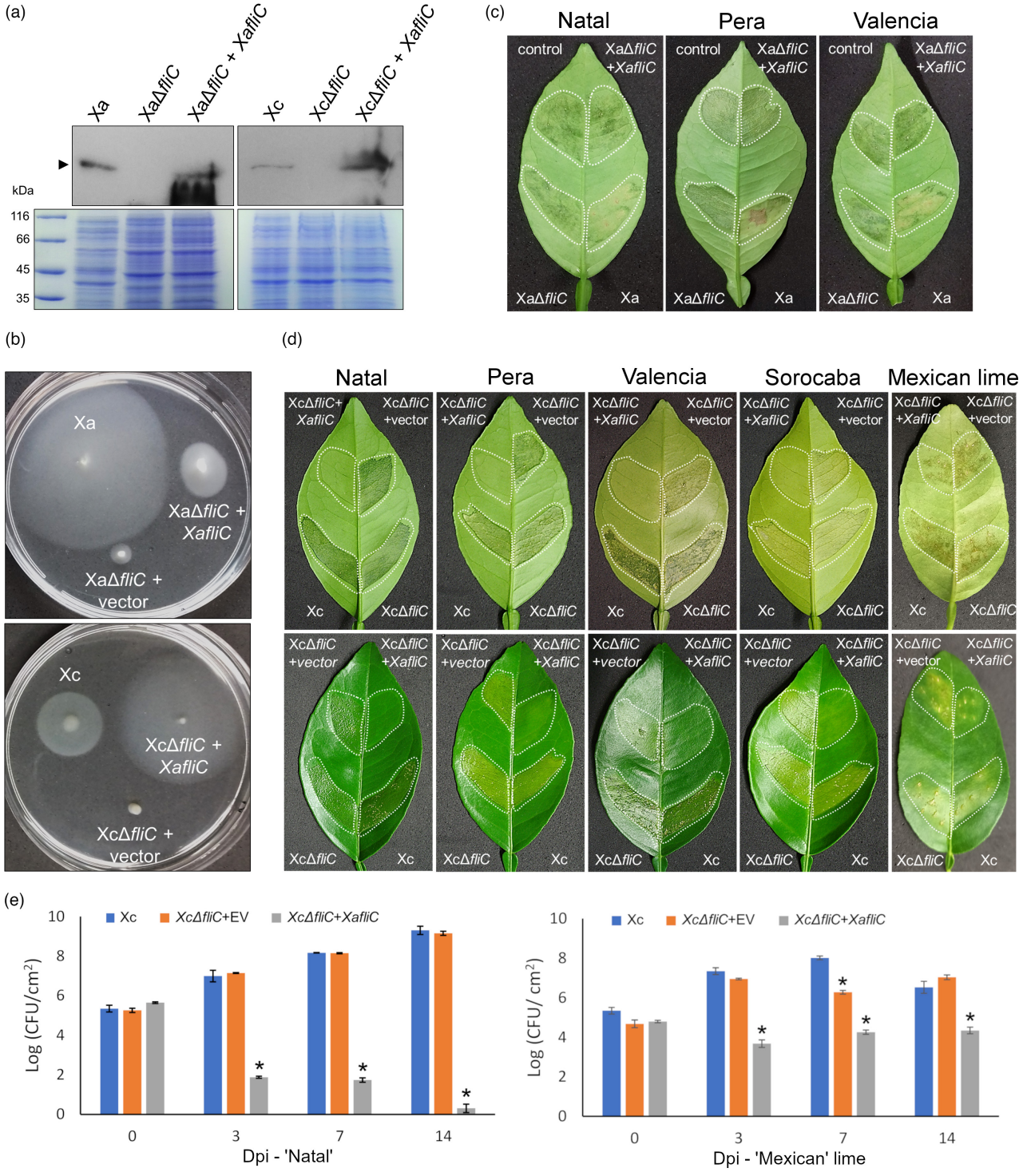

Xc preferentially induced the expression of genes associated with canker formation, including *CsLOB1*, Xa rapidly induced the expression of *FLS2* and *WRKY22*, suggesting that flagellin perception was predominantly activated by this bacterium (Data S1).

To validate the RNA-seq data and reveal which genes among the most induced by Xa show *XaFliC*-dependent expression, RNA samples from Natal leaves infiltrated with Xc, XcΔ*fliC*, XcΔ*fliC* complemented with *XaFliC*, or water were analysed by reverse transcription-quantitative real-time PCR (RT-qPCR), 24 h after bacterial inoculation (Figure 6). We found that among the seven *RLK* genes predominantly induced by Xa (Data S1), only three (*FLS2*, *RLK15*, and *RLKC*) showed a significant *XaFliC*-dependent up-regulation (Figure 6a). Likewise, among the six Xa-induced transcription factor-encoding genes tested, *WRKY22* and *MYB102* were the most highly induced in response to *XaFliC* expression (Figure 6b). Moreover, several Xa-induced genes related to oxidative burst (*respiratory burst oxidase homologue D* [*RBOHB*], *glutathione-S-transferase* [*GST*], and *peroxidase 52* [*PRX52*]) and the HR and senescence (*senescence-associated gene 13* [*SAG13*], *accelerated cell death 2* [*ACD2*], *plant U-box protein 24* [*PUB24*], *cytochrome P450 3A* [*CYP3A*],

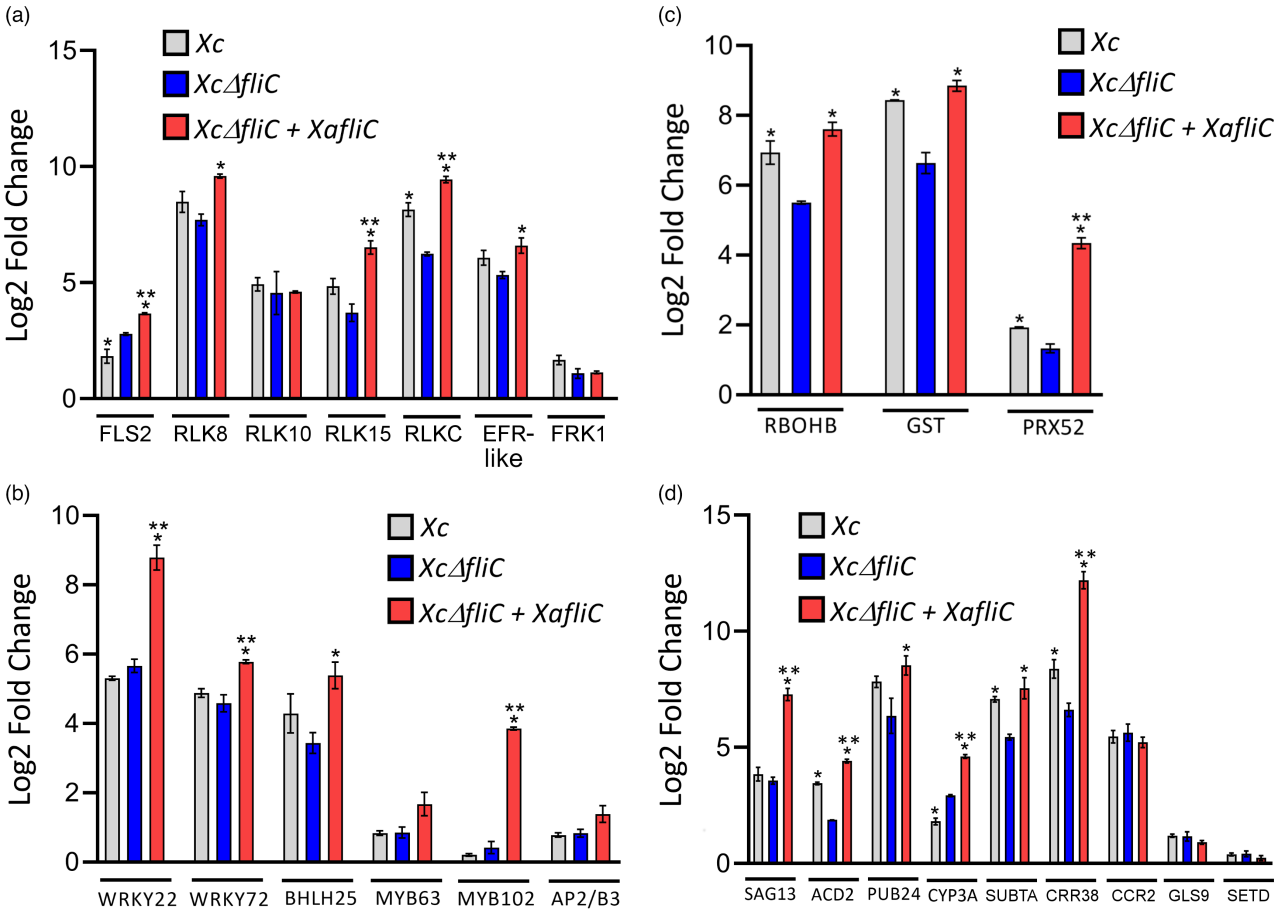

FIGURE 6 *XaFliC*-dependent expression of *FLS2*, *WRKY22*, and other defence-related genes in sweet orange. Reverse transcription-quantitative PCR analysis of Natal leaves challenged with *Xanthomonas citri* (Xc), Xc*ΔfliC*, Xc*ΔfliC* complemented with *XaFliC*, or water as control, 24 h after bacterial inoculation. (a) Relative expression levels of *RLK* genes showing *XaFliC*-dependent expression of *Xanthomonas aurantifolii* (Xa)-induced genes, including *FLS2*. (b) Relative expression levels of transcription factor-encoding genes showing that the *WRKY22* and *MYB102* homologues are the most highly up-regulated in response to *XaFliC* expression. (c) Relative expression levels of oxidative burst-associated genes showing significant induction of the putative peroxidase gene *PRX52* in leaves infiltrated with Xc*ΔfliC* complemented with *XaFliC* relative to leaves infiltrated with Xc or Xc*ΔfliC*. (d) Relative expression levels of hypersensitive response (HR)- and senescence-related genes showing *XaFliC*-dependent expression of the *SAG13*, *ACD2*, *CYP3A*, and *CRR38* homologues. Error bars represent standard deviations of three independent biological samples, whereas asterisks denote statistically significant differences between the means at the $\alpha = 0.05$ level relative to Xc*ΔfliC* (*) or Xc (**)

and *cysteine-rich repeat protein 38* [*CRR38*]) also showed *XaFliC*-dependent up-regulation (Figure 6c,d, respectively). This pattern of gene regulation is thus consistent with the fact that *XaFliC* triggers a basal defence response in sweet oranges.

To know whether flgIII-20 and flgIII-27 from *XaFliC* could also induce the expression of the citrus genes up-regulated by *XaFliC* (Figure 6), we performed RT-qPCR analysis of Natal leaves infiltrated with these peptides. Considering that flg22 induces rapid activation of gene expression in plant cells with maximum transcriptional changes occurring for instance in *Arabidopsis* at 3 h after treatment (Czékus et al., 2021; Denoux et al., 2008), we inspected the mRNA levels of the *XaFliC*-induced genes (Figure 6) in Natal leaves 3 h after leaves had been infiltrated with flgIII-20 or flgIII-27 from *XaFliC* and *XcFliC*, or with flg22 or water as controls. Although flgIII-20 did not significantly change the expression levels of the *XaFliC*-induced genes analysed, except for a small induction of *FLS2*, *WRKY22*, and *MYB102* caused by flgIII-20 from *XaFliC* only, we found that flgIII-27 from *XaFliC*, but not *XcFliC*, specifically induced the expression of *FLS2*, *RLK15*, *RLKC*, *FRK1*, *CRR38*, *bHLH25*, *MYB102*, *SAG13*, and *ACD2*, relative to water infiltration (Figure 7). In addition, except for *FLS2*, all these genes were more strongly up-regulated in response to flgIII-27 than in response to flg22 (Figure 7). Surprisingly, *WRKY22* and *WRKY72* were equally induced by flgIII-27 from *XaFliC* and *XcFliC* (Figure 7).

2.7 | Amino acid polymorphisms of flgIII-20 and flgIII-27 are commonly found in the *Xanthomonas* genus

To analyse whether the polymorphisms observed between *XaFliC* and *XcFliC* are conserved among Xc and Xa strains or also found in

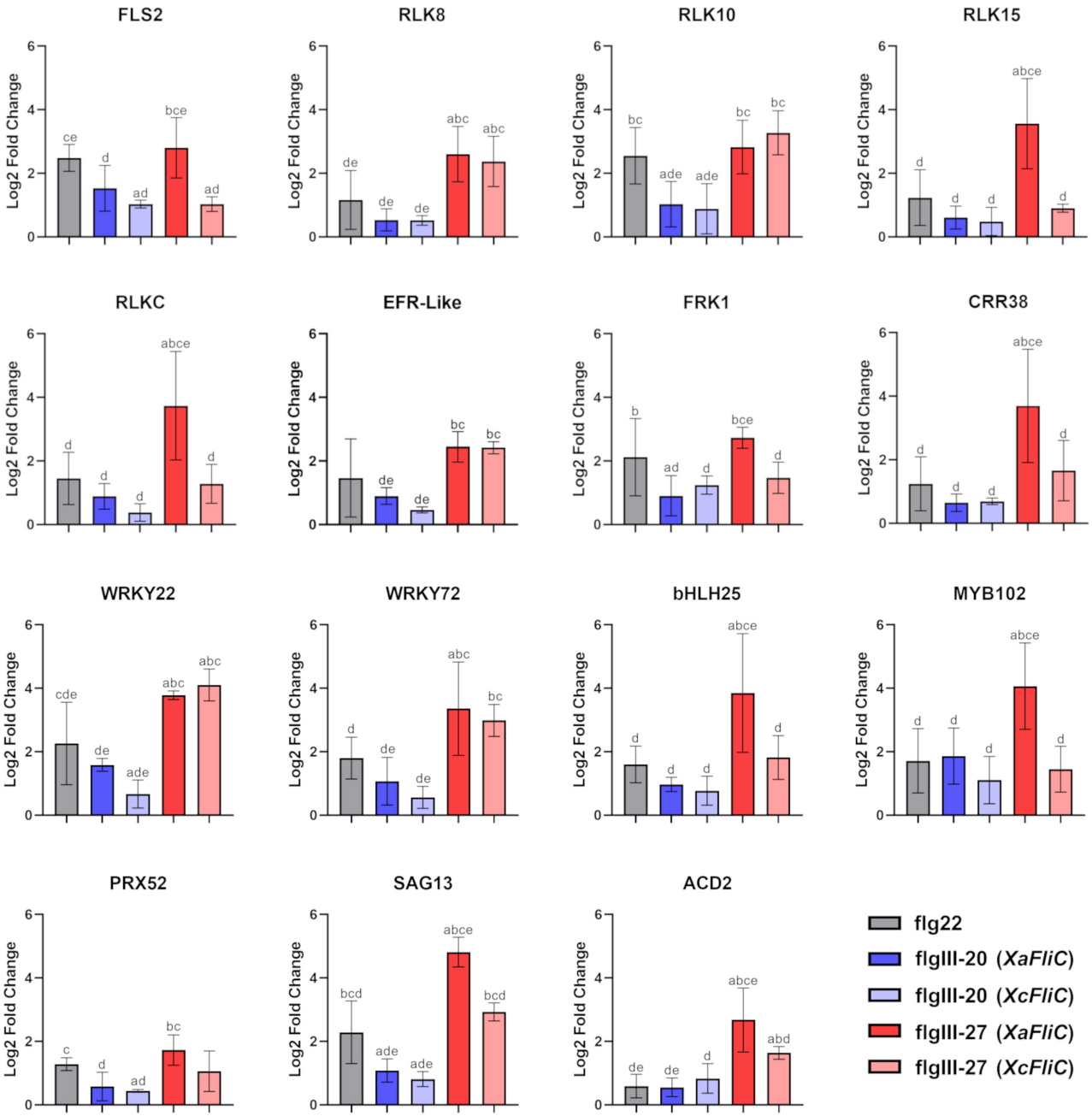

FIGURE 7 Gene expression analysis of *XaFliC*-induced genes in response to treatment with flg peptides. Reverse transcription-quantitative PCR analysis of Natal leaves infiltrated with 70 μM flgIII-20 or flgIII-27 from *XaFliC* and *XcFliC*, or with flg22 or water, used as controls, 3 h postinfiltration. While flgIII-20 did not significantly change the expression levels of most *XaFliC*-induced genes, flgIII-27 from *XaFliC*, but not *XcFliC*, specifically induced the expression of *FLS2*, *RLK15*, *RLKC*, *FRK1*, *CRR38*, *bHLH25*, *MYB102*, *SAG13*, and *ACD2*, relative to the water control. Error bars denote standard deviations of two independent biological samples with three technical replicates of each treatment. Statistically significant differences among the groups are indicated by the letters a, b, c, d, and e, which represent flg22, flgIII-20 (*XaFliC*), flgIII-20 (*XcFliC*), flgIII-27 (*XaFliC*), and flgIII-27 (*XcFliC*) treatments, respectively, where a indicates, for instance, that the analysed group is statistically different ($p < 0.05$) from the flg22 treatment group

other *Xanthomonas* species/pathovars, we initially performed BlastP searches using *XaFliC* as query. Notably, we found that the amino acid sequence of *XaFliC* is fully conserved in all the designated *X. aurantifolii*, *X. citri* pv. *aurantifolii*, *X. fuscans* pv. *aurantifolii*, and *X. citri* pv. *fuscans* strains, but not in the X. *citri* pv. *citri* or *Xanthomonas axonopodis* pv. *citri* strains. The NCBI accession WP_007962409 refers to 109 proteins identical to *XaFliC* belonging to several *Xanthomonas* species/pathovars most closely related to Xa, including *X. citri* pv. *phaseoli* var. *fuscans* and *Xanthomonas phaseoli* pv. *dieffenbachiae*. Likewise, BlastP searches using *XcFliC* as query revealed 410 identical proteins belonging mainly to *X. citri*, *X. citri* pv. *citri*, and *X. axonopodis* pv. *citri* strains and other *Xanthomonas* species, but none

belonging to *X. aurantifolii* strains (NCBI multispecies accession number WP_003482972).

Next, we performed BlastP searches using only the *XaFliC* region spanning the flgIII-20 and flgIII-27 peptides. The resulting sequence alignment comprising mostly nonidentical sequences sharing 98% to 65% identity to *XaFliC* is shown in Figure 8. This protein alignment confirms that the amino acid polymorphism found between *XaFliC* and *XcFliC* is shared among many *Xanthomonas* species/pathovars, suggesting that the *FliC* regions spanning flgIII-20 and flgIII-27 are subject to selective pressure. This assumption is supported by the type of amino acid changes observed at specific positions in these regions. For instance, in flgIII-20, a K-to-D change at position 6 and an S/T-to-N change at position 10 distinguish a large group of *Xanthomonas* species/pathovars, including Xa, from the *X. citri*, *Xanthomonas passiflorae*, *Xanthomonas manihotis*, and *Xanthomonas malvacearum* group (Figure 8). It is expected that only these two nonconserved amino acid changes could potentially alter recognition or affinity of flgIII-20 by a pattern recognition receptor (PRR). Likewise, the nonconserved changes from S to V at position 6 and from S/G/A to T at position 9 in flgIII-27 also distinguish the Xa-related group from the Xc-related group (Figure 8). Furthermore, two serine residues, at positions 10 and 17 in flgIII-27, are replaced by N/D and A, respectively, between these two groups of *Xanthomonas*, except in *Xanthomonas fragariae*, which has an asparagine residue at position 10 (Figure 8). Because serine and threonine residues are prone to phosphorylation and glycosylation (Nothaft & Szymanski, 2010; Shi et al., 2014), such substitutions may represent important changes in the *FliC* structure and consequently receptor recognition.

3 | DISCUSSION

Understanding how plants perceive and defend themselves from pathogen attack is of paramount importance for crop protection and

FIGURE 8 Amino acid polymorphisms in flgIII-20 and flgIII-27 are found in several *Xanthomonas* species and pathovars. Protein sequence alignment of *Xanthomonas FliC* proteins showing that the amino acid polymorphisms found in flgIII-20 and flgIII-27 between *Xanthomonas aurantifolii* (Xa) and *X. citri* (Xc) are also present in several species/pathovars of *Xanthomonas*. The alignment, performed with ClustalW, includes the *FliC* regions spanning the flgIII-20 and flgIII-27 peptides from the following *Xanthomonas* species/pathovars: Xa (WP_007962409), *X. citri* pv. *glycines* WP_016848727, *X. campestris* pv. *mirabilis* WP_218495416, *X. euvesicatoria* WP_218195708, *X. euvesicatoria* pv. *allii* MCP3041826, *X. citri* pv. *thirumalacharii* WP_223574663, *X. campestris* pv. *paulliniae* WP_218557524, *X. arboricola* WP_055854457, *X. perforans* MCF5971967, *X. dyei* WP_104616676, *X. prunicola* WP_101364107, *X. oryzae* WP_134953848, *X. oryzae* pv. *oryzicola* AEQ96507, *X. fragariae* WP_254223128, *X. hortorum* WP_115038939, *X. pisi* WP_046964182, *X. floridensis* WP_064510802, *X. cucurbitae* WP_104603719, *X. cannabis* WP_047696158.1, *X. bromi* WP_065467843, *X. vesicatoria* WP_005994319, *X. campestris* WP_218559892, *X. vasicola* WP_010373629, *X. axonopodis* pv. *passiflorae* MBV6815034, *X. axonopodis* pv. *manihotis* WP_017154654, *X. citri* pv. *malvacearum* WP_003482972.1, and Xc (WP_003482972). A K-to-D change at position 6 and an S/T-to-N change at position 10 in flgIII-20 distinguish a large group of *Xanthomonas* species/pathovars, including Xa, from the *citri*, *passiflorae*, *manihotis*, and *malvacearum* group. The nonconserved changes from S to V at position 6 and from S/G/A to T at position 9 in flgIII-27 also distinguish the Xa-related group from the Xc-related group. Two serine residues at positions 10 and 17 in flgIII-27 are replaced by N/D and A, respectively, between the Xa- and Xc-related groups, except in *X. fragariae*, which has an asparagine residue at position 10

food security. In this study, we unravelled the molecular basis underlying the immune response triggered by Xa in sweet orange plants, which for a long time remained a mystery to plant pathologists.

We show here that the *XaFliC* protein is sufficient to induce a robust defence response in several sweet orange varieties and Troyer citrange plants, protecting them against Xc infection. We also show that two polymorphic *XaFliC* peptides, flgIII-20 and flgIII-27, which belong to the structural domain D2, inhibited Xc-induced canker development more pronouncedly in orange cultivars than in Mexican lime, indicating that *XaFliC* acts as a PAMP in sweet oranges.

The identification of *XaFliC* as a major elicitor that triggers an immune response in sweet oranges during Xa infection is in line with the fact that none of the *PthA* effectors from Xa strains act as avirulence factors in sweet orange cultivars (Al-Saadi et al., 2007; Brunings & Gabriel, 2003), which thus characterize this defence mechanism as PAMP- and not effector-triggered immunity. Additionally, although amino acid and glycosylation polymorphisms in *FliC* proteins have been well documented as plant defence evasion mechanisms exploited by many bacterial pathogens (Buscaill et al., 2019; Hirai et al., 2011; Malvino et al., 2022; Sun et al., 2006; Wang et al., 2015; Wei et al., 2020), to the best of our knowledge, this is the first description of amino acid polymorphisms among *FliC* proteins of citrus canker bacteria determining the host range. Furthermore, such polymorphisms were found in peptide regions other than flg22 and flgII-28, the only known *FliC* peptides and the best-characterized PAMPs recognized by FLS receptors (Cai et al., 2011; Clarke et al., 2013; Gomez-Gomez & Boller, 2002; Hind et al., 2016; Zipfel et al., 2004). Importantly, we found no *FliC* protein belonging to *X. aurantifolii* strains carrying the amino acid substitutions of flgIII-20 and flgIII-27 of *XcFliC*. Likewise, no *FliC* protein belonging to *X. citri* strains carries the amino acid substitutions of flgIII-20 and flgIII-27 of *XaFliC*. Nevertheless, the polymorphisms found in flgIII-20 and flgIII-27 between Xa and Xc are found in many *Xanthomonas* species/pathovars. Furthermore, the nonconserved amino acid exchanges found in flgIII-20 and flgIII-27 between *XaFliC* and *XcFliC* are expected to significantly alter the affinity to or the recognition by a PRR. Thus, our data suggest that these regions are under selective pressure and that the flgIII-20 and flgIII-27 polymorphisms could contribute to plant immunity evasion. Interestingly, the region covering the *FliC* D2 domain of the rice pathogen *Acidovorax avenae*, carrying the corresponding flgIII-20 and flgIII-27 peptides, also induced an immune response in *Oryza sativa*, *Brachypodium distachyon*, and *Asparagus persicus* (Katsuragi et al., 2015; Murakami et al., 2022).

Consistent with its role as a PAMP, ectopic expression of *XaFliC* in the Xc*ΔfliC* mutant led to the up-regulation of several defence-related genes also induced by Xa in sweet orange plants. Many of such genes that displayed a robust induction in a *XaFliC*-dependent manner, including the citrus homologues *FLS2*, *WRKY22*, *ACD2*, *PRX52*, and *SAG13*, are typically induced in incompatible plant–pathogen interactions. For instance, the *Arabidopsis ACD2* gene, which encodes the red chlorophyll catabolite enzyme, not only delays plant cell death, but also modulates the onset of HR affecting pathogen survival during bacterial infection (Yao & Greenberg, 2006). This type of response is reminiscent of what is normally observed in sweet orange leaves infected with Xa, where necrosis or extensive plant cell death is atypical (Cernadas et al., 2008). Moreover, the *XaFliC*-induced *PRX52* gene encodes a protein related to *C. sinensis* CsPRX25, an apoplastic peroxidase implicated in ROS homeostasis and cell wall lignification that confers resistance against Xc when overexpressed in transgenic citrus (Li et al., 2020). This is particularly important because lignification of the cell wall is a hallmark of Xa infection in sweet orange leaves (Cernadas et al., 2008). Furthermore, in addition to *SAG13*, a gene that is rapidly induced during HR in response to avirulent *Pseudomonas syringae* and flg22 (Dhar et al., 2020), the concomitant up-regulation of the transcription factor genes *bHLH25* and *MYB102* by *XaFliC* is of particular interest because these transcriptional factors can form heterodimers to regulate distinct cellular processes, including defence (Pireyre & Burow, 2015).

In line with the results of gene induction mediated by *XaFliC*, *FLS2*, *WRKY22*, and *MYB102* showed a slight induction in response to flgIII-20, whereas *FLS2*, *RLK15*, *RLKC*, *FRK1*, *CRR38*, *bHLH25*, *MYB102*, *SAG13*, and *ACD2* were greatly up-regulated by flgIII-27, thus supporting the idea that flgIII-20 and flgIII-27 from XaFliC, but not *XcFliC*, act as PAMPs in sweet oranges. In fact, activation of most *XaFliC*-induced genes was more pronounced in response to flgIII-27 than in response to flg22.

The observation that activation of FLS2 by flg22 leads to rapid degradation with subsequent de novo mRNA accumulation and synthesis of the receptor (Smith et al., 2014) suggests that up-regulation of *PRR* genes in plants can occur in response to receptor activation after ligand binding. Based on this premise and on our gene expression data, we consider that the citrus FLS2-1, RLK15, and RLKC proteins could represent potential PRR candidates to recognize flgIII-20 or flgIII-27. For instance, the citrus *FLS2* gene, which is up-regulated in response to *XaFliC*, flgIII-20, and flgIII-27, corresponds to the *FLS2-1* allele (GenBank XP_006478775) firstly characterized in Duncan grapefruit and shown to be induced by Xc flg22 (Hao et al., 2016; Shi et al., 2016, 2018). However, considering that the FLS2-1 protein has not yet been demonstrated to bind flg22 with high affinity and that the *Arabidopsis* FLS2 receptor recognizes an array of flg22 variants to tune the immune response against pathogens and commensal bacteria (Colaianni et al., 2021; Parys et al., 2021; Stringlis & Pieterse, 2021), one cannot rule out the possibility that FLS2-1 could sense flgIII-20 or flgIII-27. Likewise, the citrus RLK15, RLKC, and CRR38 proteins, which were more pronouncedly induced by flgIII-27 than by flg22, also remain as possible receptor candidates for flgIII-27 perception. In particular, citrus CRR38 belongs to the subfamily of plant RLKs that contain two C-X_8-C-X_2-C motives and are referred to as cysteine-rich receptor-like secreted proteins (Vaattovaara et al., 2019). However, CRR38 harbours a predicted transmembrane helix at the N-terminus, suggesting that it might be surface-localized and attached to the cell membrane. CRR38 is related to *Arabidopsis* CRK28, a membrane receptor induced by flg22 and whose enhanced expression increases disease resistance against *P. syringae*. Notably, CRK28 is associated with BAK1 and was detected

in the FLS2–BAK1 immune complex (Yadeta et al., 2017). Therefore, because plant CRK receptors are thought to sense a diverse set of ligands (Vaattovaara et al., 2019), it is possible that CRR38 could act in conjunction with FLS2-1, RLK15, or RLKC to sense flgIII-27. In fact, the citrus RLKC protein belongs to the family of lectin receptor-like kinases recently found to play crucial roles in PAMP recognition and plant defence (Luo et al., 2017; Sun et al., 2020; Wang & Bouwmeester, 2017). Although further studies will be needed to demonstrate whether any of these PRR candidates recognizes the *XaFliC* polymorphic peptides to trigger the immune response in sweet oranges, we believe this work provides a better understanding of the molecular players involved in such defence mechanism, which may support the development of new approaches to protect citrus plants from bacterial pathogens.

4 | EXPERIMENTAL PROCEDURES

4.1 | Bacterial strains and generation of *fliC* mutants

X. citri (strain 306) and *X. aurantifolii* pathotype C (strain ICMP 8435) were grown in LBON medium supplemented with 100 mg/L ampicillin for 48 h at 28°C (Cernadas et al., 2008). XcΔ*fliC* and XaΔ*fliC* mutants were generated as previously described (Andrade et al., 2014). Briefly, DNA fragments of approximately 1 kb flanking the *XcFliC* coding region were amplified using a high-fidelity polymerase (Phusion; Thermo Scientific) and cloned into the *Hin*dIII site of the pNPTS138 vector. To generate the *XaFliC* knockout mutant, a 0.5-kb DNA fragment encoding only the central region of the *XaFliC* gene was amplified and cloned into the *Hin*dIII site of pNPTS138. The resulting constructs pNPTS-XcΔ*fliC* and pNPTS-XaΔ*fliC* were used to transform Xc and Xa cells by electroporation. The wild-type copies of *XcFliC* and *XaFliC* were replaced with the respective deleted versions of the genes after two recombination events. All mutant clones were confirmed using PCR. To complement the XcΔ*fliC* and XaΔ*fliC* mutants, the *XaFliC* coding sequence was amplified by PCR using genomic DNA extracted from wild-type Xa as template. The amplified fragment was cloned into pUFR053 at the *Bam*HI and *Hin*dIII restriction sites to obtain the recombinant plasmid pUFR053_*XaFliC*, which was used for genetic complementation. The construction was transferred into both mutant strains using electroporation, and cells were selected using 10 μg/ml gentamicin. The oligonucleotides used for producing the *fliC* mutant constructs are listed in Table S2.

4.2 | Plant growth and bacterial inoculations

The sweet orange (*C. sinensis*) varieties Natal, Pera, Valencia, and Sorocaba and the Mexican lime (*C. aurantifolia*) cultivar Galego were obtained from certified nurseries and kept in a greenhouse. Plant leaves were infiltrated with water suspensions of Xc, Xa, the corresponding *fliC* mutants, or mixed suspensions of Xa and Xc or Xc and XaΔ*fliC* at a 1:1 ratio (OD_{600} = 0.1). Single colonies of Xc, Xa, or corresponding *fliC* mutants were suspended in sterile water to a final OD_{600} of 0.05 or 0.1 for leaf infiltration. Citrus leaves were also infiltrated with a water suspension of Xc (OD_{600} = 0.05) in the presence of FliC peptides at a final concentration of 70 μM. Canker symptoms were typically recorded 10 to 15 days after bacterial inoculation.

4.3 | Bacterial growth analysis

The growth of Xc and corresponding XcΔ*fliC* mutants complemented with *XaFliC* or with the empty vector were analysed in Natal and Mexican lime leaves. Discs of 0.5 cm in diameter were removed from leaf sectors infiltrated with a water suspension of bacterial cells (OD_{600} = 0.2) at different time intervals after bacterial inoculation and macerated in 1 ml of sterile water. Tenfold serial dilutions of the bacterial suspensions were plated on LBON supplemented with ampicillin, and bacterial colonies were counted from three independent leaf extractions. Statistical analyses were performed with one-way analysis of variance (ANOVA) followed by Bonferroni's test for multiple comparisons ($p < 0.05$).

4.4 | *FliC* identification and peptide mapping

Bacterial cells were grown in liquid LBON supplemented with ampicillin for 18 h at 28°C under mild agitation (100 rpm). Cells were collected by centrifugation (5000 × *g*) at 4°C for 5 min and suspended in 25 mM Tris–HCl, 150 mM NaCl, pH 7.0. The suspensions were homogenized in a cell mixer (Politron PT-MR 1600 E) for 5 min on ice. Bacterial cells were recovered by centrifugation and the suspensions containing bacterium flagellum were precipitated with acetone (at a 1:1 ratio) at −20°C overnight. The suspensions were centrifuged (5000 × *g*) at 4°C for 10 min and the protein pellets were suspended in SDS-PAGE sample buffer and resolved on 10% SDS-PAGE gels. Protein bands were extracted from the gels and digested with trypsin, and the cleaved peptides were identified by mass spectrometry, as previously described (Soprano et al., 2017). The mass spectrometry proteomic data have been deposited to the ProteomeXchange Consortium via the PRIDE partner repository (Perez-Riverol et al., 2022) with the dataset identifier PXD037760.

4.5 | Protein sequence alignment and molecular modelling

Protein sequence alignments were performed with Clustal Omega using default parameters, whereas 3D structural models of the *FliC* proteins were generated with SWISS-MODEL using the crystal structure of the *Sphingomonas* sp. A1 flagellin (PDB code 3K8V) as a template model. The structures were visualized and compared using PyMOL (Schrodinger, LLC, 2015).

4.6 | Bacterial motility assays

Bacterial motility assays were performed as previously described (Andrade et al., 2020). Briefly, cells grown in LBON plus 1.5% (wt/vol) agar for 48 h at 28°C were stabbed into 0.3% (wt/vol) agar nutrient broth medium plates. Motility was evaluated and bacteria were photographed after 3 days of incubation at 28°C. The assays were performed with three independent replicates.

4.7 | *FliC* purification and antibody production

The *XaFliC* gene was cloned into the pET28a vector for the expression of recombinant 6×His-tagged *XaFliC* in *Escherichia coli* BL21(DE3) cells. Bacterial cells were grown in Luria-Bertani medium supplemented with kanamycin (50 mg/L) at 37°C and protein expression was induced with 0.1 mM IPTG for 3 h under agitation (200 rpm). Bacterial cells were suspended in 50 mM Tris–HCl, pH 8.0, 300 mM NaCl, 5 mM imidazole, lysed with lysozyme (1 mg/ml) and sonication, and centrifuged at 18,000×*g* at 4°C for 30 min. The recombinant protein in the soluble fraction was purified by affinity chromatography and eluted with 50 mM Tris–HCl, pH 8.0, 300 mM NaCl, 250 mM imidazole. Fractions containing the recombinant XaFliC were pooled, concentrated, and fractionated on a Superdex 200 10/30 column equilibrated with 50 mM Tris–HCl, pH 8.0, 300 mM NaCl. Fractions containing purified XaFliC were concentrated and used to immunize white rabbits for antibody production (Rhea Biotech, Campinas, Brazil).

4.8 | Western blot analyses

Xc and Xa cells were suspended in SDS-PAGE sample buffer and incubated at 90°C for 5 min for cell disruption. Cell debris was pelleted by centrifugation at 15,000×*g* for 5 min and the supernatants were resolved by 10% SDS-PAGE. The proteins were transferred to PVDF membranes, which were blocked with skimmed milk and probed with the primary anti-*XaFliC* antibodies (1:1000) overnight at 4°C under mild agitation. After washing with phosphate-buffered saline, the membranes were incubated with horseradish peroxidase-conjugated secondary anti-rabbit IgG (GE Healthcare) at 1:3000 dilution for 3 h at room temperature with mild agitation. Protein bands were detected by chemiluminescence with Super Signal West Pico Chemiluminescent substrate (Thermo Scientific).

4.9 | RNA-seq and gene expression analysis

Natal leaves of similar size and age were infiltrated with water suspensions of Xc or Xa (OD_{600} = 0.1), or water as control. The infiltrated leaf sectors were collected at 24 and 48 h after bacterial infiltration and immediately frozen in liquid nitrogen. Leaf tissues were ground in liquid nitrogen and total RNA was extracted from three independent leaves using TRIzol reagent (Invitrogen). The quality and quantity of the RNA samples were verified by NanoDrop measurements and agarose gels. The RNA samples were treated with DNase I to remove traces of DNA and subjected to HISEQ2500 Illumina sequencing at the LaCTAD facility of the State University of Campinas. Reads of each sample (28,000,000 on average) were aligned with the *C. sinensis* transcripts of the Phytozome database using the RSEM program (Li & Dewey, 2011), which allowed the mapping of more than 20,000,000 reads per sample, and the output files were recorded in bam format (Li et al., 2009; Mortazavi et al., 2008). The expression value of each transcript (FPKM) was calculated using RSEM according to Mortazavi et al. (2008). The RNA-seq data were deposited in the GEO database with the following accession numbers: GSE202469 and GSM6122945 to GSM6122959.

For RT-qPCR analyses, leaves of Natal plants were infiltrated with Xc, XcΔ*fliC*, XcΔ*fliC* complemented with the *XaFliC* gene, or water as control. Total RNA was extracted from the infiltrated leaf sectors 24 h after bacterial inoculation. In addition, Natal leaves were infiltrated with water suspensions of the flg peptides at a final concentration of 70 μM, and total RNA was extracted 3 h after peptide inoculation. RNA extraction followed by mRNA purification and RT-qPCR were performed as described previously (Andrade et al., 2020). The oligonucleotides used for the amplification of the citrus genes are listed in Table S2. Gene expression values were normalized using the *GAPDH* gene as endogenous control and three independent biological replicates were evaluated for all treatments. Fold change values were calculated using the $2^{-\Delta\Delta Ct}$ method (Livak & Schmittgen, 2001). Statistical analyses were conducted with one-way ANOVA followed by Dunnett's and Tukey's tests for multiple comparisons ($p < 0.05$).

ACKNOWLEDGEMENTS

We acknowledge the use of the LNBio facilities LPP and MAS for protein production and mass spectrometry analysis, respectively. We thank Jackeline Zanella, Romenia Domingues, and Bianca Pauletti for technical help. We also thank Dr Marcelo Falsarella Carazzolle for helping us with the initial analysis of the RNA-seq data. This work was supported by the São Paulo Research Foundation – FAPESP (grants 2020/02547-0, 2018/08535-4, and 2014/50880-0 and fellowship 2013/22507-0 to H.M.S. and fellowship 2017/18570-9 to M.O.A.), the Ministry of Science, Technology and Innovation, and the Conselho Nacional de Desenvolvimento Científico e Tecnológico – CNPq (fellowships 303238/2016-0 to C.E.B. and 164832/2017-3 to M.O.A.).

DATA AVAILABILITY STATEMENT

The data that support the findings of this study are available from the corresponding author upon reasonable request. The RNA-seq data are openly available in the GEO repository at https://www.ncbi.nlm.nih.gov/geo/ with the following reference numbers: GSE202469 and GSM6122945 to GSM6122959. The mass spectrometry proteomic data have been deposited to the ProteomeXchange Consortium at http://www.proteomexchange.org via the PRIDE partner repository (Perez-Riverol et al., 2022) with the dataset identifier PXD037760.

ORCID

Celso Eduardo Benedetti https://orcid.org/0000-0002-4602-0256

REFERENCES

Abe, V.Y. & Benedetti, C.E. (2016) Additive roles of PthAs in bacterial growth and pathogenicity associated with nucleotide polymorphisms in effector-binding elements of citrus canker susceptibility genes. *Molecular Plant Pathology*, 17, 1223–1236.

Al-Saadi, A., Reddy, J.D., Duan, Y.P., Brunings, A.M., Yuan, Q. & Gabriel, D.W. (2007) All five host-range variants of *Xanthomonas citri* carry one pthA homolog with 17.5 repeats that determines pathogenicity on citrus, but none determine host-range variation. *Molecular Plant-Microbe Interactions*, 20, 934–943.

Andrade, M.O., Farah, C.S. & Wang, N. (2014) The post-transcriptional regulator rsmA/csrA activates T3SS by stabilizing the 5' UTR of hrpG, the master regulator of *hrp/hrc* genes, in Xanthomonas. *PLoS Pathogens*, 10, e1003945.

Andrade, M.O., Pang, Z., Achor, D.S., Wang, H., Yao, T., Singer, B.H. et al. (2020) The flagella of '*Candidatus* Liberibacter asiaticus' and its movement in planta. *Molecular Plant Pathology*, 21, 109–123.

Brunings, A.M. & Gabriel, D.W. (2003) *Xanthomonas citri*: breaking the surface. *Molecular Plant Pathology*, 4, 141–157.

Buscaill, P., Chandrasekar, B., Sanguankiattichai, N., Kourelis, J., Kaschani, F., Thomas, E.L. et al. (2019) Glycosidase and glycan polymorphism control hydrolytic release of immunogenic flagellin peptides. *Science*, 364, eaav0748.

Cai, R., Lewis, J., Yan, S., Liu, H., Clarke, C.R., Campanile, F. et al. (2011) The plant pathogen *Pseudomonas syringae* pv. *tomato* is genetically monomorphic and under strong selection to evade tomato immunity. *PLoS Pathogens*, 7, e1002130.

Cernadas, R.A., Camillo, L.R. & Benedetti, C.E. (2008) Transcriptional analysis of the sweet orange interaction with the citrus canker pathogens *Xanthomonas axonopodis* pv. *citri* and *Xanthomonas axonopodis* pv. *aurantifolii*. *Molecular Plant Pathology*, 9, 609–631.

Clarke, C.R., Chinchilla, D., Hind, S.R., Taguchi, F., Miki, R., Ichinose, Y. et al. (2013) Allelic variation in two distinct *Pseudomonas syringae* flagellin epitopes modulates the strength of plant immune responses but not bacterial motility. *The New Phytologist*, 200, 847–860.

Colaianni, N.R., Parys, K., Lee, H.S., Conway, J.M., Kim, N.H., Edelbacher, N. et al. (2021) A complex immune response to flagellin epitope variation in commensal communities. *Cell Host & Microbe*, 29, 635–649.e9.

Czékus, Z., Kukri, A., Hamow, K.Á., Szalai, G., Tari, I., Ördög, A. et al. (2021) Activation of local and systemic defence responses by flg22 is dependent on daytime and ethylene in intact tomato plants. *International Journal of Molecular Sciences*, 22, 8354.

Denoux, C., Galletti, R., Mammarella, N., Gopalan, S., Werck, D., De Lorenzo, G. et al. (2008) Activation of defense response pathways by OGs and Flg22 elicitors in *Arabidopsis* seedlings. *Molecular Plant*, 1, 423–445. Erratum in: Molecular Plant, 2009 2, 838.

Dhar, N., Caruana, J., Erdem, I., Subbarao, K.V., Klosterman, S.J. & Raina, R. (2020) The *Arabidopsis* SENESCENCE-ASSOCIATED GENE 13 regulates dark-induced senescence and plays contrasting roles in defense against bacterial and fungal pathogens. *Molecular Plant-Microbe Interactions*, 33, 754–766.

Duan, S., Jia, H., Pang, Z., Teper, D., White, F., Jones, J. et al. (2018) Functional characterization of the citrus canker susceptibility gene CsLOB1. *Molecular Plant Pathology*, 198), 1908–1916.

Fonseca, N.P., Patane, J.S.L., Varani, A.M., Felestrino, E.B., Caneschi, W.L., Sanchez, A.B. et al. (2019) Analyses of seven new genomes of *Xanthomonas citri* pv. *aurantifolii* strains, causative agents of citrus canker B and C, show a reduced repertoire of pathogenicity-related genes. *Frontiers in Microbiology*, 10, 2361.

Gochez, A.M., Minsavage, G.V., Potnis, N., Canteros, B.I., Stall, R.E. & Jones, J.B. (2015) Functional XopAG homologue in *Xanthomonas fuscans* pv. *aurantifolii* strain C limits host range. *Plant Pathology*, 64, 1207–1214.

Gochez, A.M., Shantharaj, D., Potnis, N., Zhou, X., Minsavage, G.V., White, F.F. et al. (2017) Molecular characterization of XopAG effector AvrGf2 from *Xanthomonas fuscans* ssp. *aurantifolii* in grapefruit. *Molecular Plant Pathology*, 18, 405–419.

Gomez-Gomez, L. & Boller, T. (2002) Flagellin perception: a paradigm for innate immunity. *Trends in Plant Science*, 7, 251–256.

Graham, J.H., Gottwald, T.R., Cubero, J. & Achor, D.S. (2004) *Xanthomonas axonopodis* pv. *citri*: factors affecting successful eradication of citrus canker. *Molecular Plant Pathology*, 5, 1–15.

Hao, G., Pitino, M., Duan, Y. & Stover, E. (2016) Reduced susceptibility to *Xanthomonas citri* in transgenic citrus expressing the FLS2 receptor from *Nicotiana benthamiana*. *Molecular Plant-Microbe Interactions*, 29, 132–142.

Hind, S.R., Strickler, S.R., Boyle, P.C., Dunham, D.M., Bao, Z., O'Doherty, I.M. et al. (2016) Tomato receptor FLAGELLIN-SENSING 3 binds flgII-28 and activates the plant immune system. *Nature Plants*, 2, 16128.

Hirai, H., Takai, R., Iwano, M., Nakai, M., Kondo, M., Takayama, S. et al. (2011) Glycosylation regulates specific induction of rice immune responses by *Acidovorax avenae* flagellin. *Journal of Biological Chemistry*, 286, 25519–25530.

Hu, Y., Zhang, J., Jia, H., Sosso, D., Li, T., Frommer, W.B. et al. (2014) Lateral organ boundaries 1 is a disease susceptibility gene for citrus bacterial canker disease. *Proceedings of the National Academy of Sciences of the United States of America*, 111, E521–E529.

Katsuragi, Y., Takai, R., Furukawa, T., Hirai, H., Morimoto, T., Katayama, T. et al. (2015) CD2-1, the C-terminal region of flagellin, modulates the induction of immune responses in rice. *Molecular Plant-Microbe Interactions*, 28, 648–658.

Li, B. & Dewey, C.N. (2011) RSEM: accurate transcript quantification from RNA-seq data with or without a reference genome. *BMC Bioinformatics*, 12, 323.

Li, H., Handsaker, B., Wysoker, A., Fennell, T., Ruan, J., Homer, N. et al. (2009) The sequence alignment/map format and SAMtools. *Bioinformatics*, 25, 2078–2079.

Li, Q., Qin, X., Qi, J., Dou, W., Dunand, C., Chen, S. et al. (2020) CsPrx25, a class III peroxidase in Citrus sinensis, confers resistance to citrus bacterial canker through the maintenance of ROS homeostasis and cell wall lignification. *Horticulture Research*, 7, 192.

Livak, K.J. & Schmittgen, T.D. (2001) Analysis of relative gene expression data using real-time quantitative PCR and the 2(−ΔΔC(T)) method. *Methods*, 25, 402–408.

Luo, X., Xu, N., Huang, J., Gao, F., Zou, H., Boudsocq, M. et al. (2017) A lectin receptor-like kinase mediates pattern-triggered salicylic acid signaling. *Plant Physiology*, 174, 2501–2514.

Malvino, M.L., Bott, A.J., Green, C.E., Majumdar, T. & Hind, S.R. (2022) Influence of flagellin polymorphisms, gene regulation, and responsive memory on the motility of *Xanthomonas* species that cause bacterial spot disease of solanaceous plants. *Molecular Plant-Microbe Interactions*, 35, 157–169.

Mortazavi, A., Williams, B.A., McCue, K., Schaeffer, L. & Wold, B. (2008) Mapping and quantifying mammalian transcriptomes by RNA-seq. *Nature Methods*, 5, 621–628.

Murakami, T., Katsuragi, Y., Hirai, H., Wataya, K., Kondo, M. & Che, F.S. (2022) Distribution of flagellin CD2-1, flg22, and flgII-28 recognition systems in plant species and regulation of plant immune responses through these recognition systems. *Bioscience, Biotechnology, and Biochemistry*, 86, 490–501.

Nicaise, V., Roux, M. & Zipfel, C. (2009) Recent advances in PAMP-triggered immunity against bacteria: pattern recognition receptors watch over and raise the alarm. *Plant Physiology*, 150, 1638–1647.

Nothaft, H. & Szymanski, C.M. (2010) Protein glycosylation in bacteria: sweeter than ever. *Nature Reviews. Microbiology*, 8, 765–778.
de Oliveira, M.L., de Lima Silva, C.C., Abe, V.Y., Costa, M.G., Cernadas, R.A. & Benedetti, C.E. (2013) Increased resistance against citrus canker mediated by a citrus mitogen-activated protein kinase. *Molecular Plant-Microbe Interactions*, 26, 1190–1199.
Oliveira Andrade, M., Sforca, M.L., Batista, F.A.H., Figueira, A.C.M. & Benedetti, C.E. (2020) The MAF1 phosphoregulatory region controls MAF1 interaction with the RNA polymerase III C34 subunit and transcriptional repression in plants. *The Plant Cell*, 32, 3019–3035.
Parys, K., Colaianni, N.R., Lee, H.S., Hohmann, U., Edelbacher, N., Trgovcevic, A. et al. (2021) Signatures of antagonistic pleiotropy in a bacterial flagellin epitope. *Cell Host & Microbe*, 29, 620–634.e9.
Pereira, A.L., Carazzolle, M.F., Abe, V.Y., de Oliveira, M.L., Domingues, M.N., Silva, J.C. et al. (2014) Identification of putative TAL effector targets of the citrus canker pathogens shows functional convergence underlying disease development and defense response. *BMC Genomics*, 15, 157.
Perez-Riverol, Y., Bai, J., Bandla, C., Hewapathirana, S., García-Seisdedos, D., Kamatchinathan, S. et al. (2022) The PRIDE database resources in 2022: a hub for mass spectrometry-based proteomics evidences. *Nucleic Acids Research*, 50(D1), D543–D552.
Pireyre, M. & Burow, M. (2015) Regulation of MYB and bHLH transcription factors: a glance at the protein level. *Molecular Plant*, 8, 378–388.
Roeschlin, R.A., Uviedo, F., Garcia, L., Molina, M.C., Favaro, M.A., Chiesa, M.A. et al. (2019) PthA4(AT), a 7.5-repeats transcription activator-like (TAL) effector from *Xanthomonas citri* ssp. *citri*, triggers citrus canker resistance. *Molecular Plant Pathology*, 20, 1394–1407.
Schrodinger, LLC (2015) *The PyMOL molecular graphics system, Version 1.8*. Available at: https://pymol.org/2/ [Accessed 20 January 2023].
Shi, L., Pigeonneau, N., Ravikumar, V., Dobrinic, P., Macek, B., Franjevic, D. et al. (2014) Cross-phosphorylation of bacterial serine/threonine and tyrosine protein kinases on key regulatory residues. *Frontiers in Microbiology*, 5, 495.
Shi, Q., Febres, V. J., Jones, J. B. & Moore, G. A. (2016). A survey of *FLS2* genes from multiple citrus species identifies candidates for enhancing disease resistance to *Xanthomonas citri* ssp. *citri*. *Horticulture Research*, 3, 16022.
Shi, Q., Febres, V.J., Zhang, S., Yu, F., McCollum, G., Hall, D.G. et al. (2018) Identification of gene candidates associated with Huanglongbing tolerance, using '*Candidatus* Liberibacter asiaticus' flagellin 22 as a proxy to challenge citrus. *Molecular Plant-Microbe Interactions*, 31, 200–211.
Smith, J.M., Salamango, D.J., Leslie, M.E., Collins, C.A. & Heese, A. (2014) Sensitivity to Flg22 is modulated by ligand-induced degradation and de novo synthesis of the endogenous flagellin-receptor FLAGELLIN-SENSING2. *Plant Physiology*, 164, 440–454.
Soprano, A.S., Abe, V.Y., Smetana, J.H. & Benedetti, C.E. (2013) Citrus MAF1, a repressor of RNA polymerase III, binds the *Xanthomonas citri* canker elicitor PthA4 and suppresses citrus canker development. *Plant Physiology*, 163, 232–242.
Soprano, A.S., Giuseppe, P.O., Shimo, H.M., Lima, T.B., Batista, F.A.H., Righetto, G.L. et al. (2017) Crystal structure and regulation of the citrus pol III repressor MAF1 by auxin and phosphorylation. *Structure*, 25, 1360–1370.e4.
de Souza, T.A., Soprano, A.S., de Lira, N.P., Quaresma, A.J., Pauletti, B.A., Paes Leme, A.F. et al. (2012) The TAL effector PthA4 interacts with nuclear factors involved in RNA-dependent processes including a HMG protein that selectively binds poly(U) RNA. *PLoS One*, 7, e32305.
Stringlis, I.A. & Pieterse, C.M.J. (2021) Evolutionary "hide and seek" between bacterial flagellin and the plant immune system. *Cell Host & Microbe*, 29, 548–550.
Sun, W., Dunning, F.M., Pfund, C., Weingarten, R. & Bent, A.F. (2006) Within-species flagellin polymorphism in *Xanthomonas campestris* pv. *campestris* and its impact on elicitation of *Arabidopsis* FLAGELLIN SENSING2-dependent defenses. *The Plant Cell*, 18, 764–779.
Sun, Y., Qiao, Z., Muchero, W. & Chen, J.G. (2020) Lectin receptor-like kinases: the sensor and mediator at the plant cell surface. *Frontiers in Plant Science*, 11, 596301.
Teper, D., Xu, J., Pandey, S.S. & Wang, N. (2021) PthAW1, a transcription activator-like effector of *Xanthomonas citri* subsp. *citri*, promotes host-specific immune responses. *Molecular Plant-Microbe Interactions*, 34, 1033–1047.
Vaattovaara, A., Brandt, B., Rajaraman, S., Safronov, O., Veidenberg, A., Luklová, M. et al. (2019) Mechanistic insights into the evolution of DUF26-containing proteins in land plants. *Communications Biology*, 2, 56.
Wang, Y. & Bouwmeester, K. (2017) L-type lectin receptor kinases: new forces in plant immunity. *PLoS Pathogens*, 13, e1006433.
Wang, S., Sun, Z., Wang, H., Liu, L., Lu, F., Yang, J. et al. (2015) Rice OsFLS2-mediated perception of bacterial flagellins is evaded by *Xanthomonas oryzae* pvs. *oryzae* and *oryzicola*. *Molecular Plant*, 8, 1024–1037.
Wei, Y., Balaceanu, A., Rufian, J.S., Segonzac, C., Zhao, A., Morcillo, R.J.L. et al. (2020) An immune receptor complex evolved in soybean to perceive a polymorphic bacterial flagellin. *Nature Communications*, 11, 3763.
Yadeta, K.A., Elmore, J.M., Creer, A.Y., Feng, B., Franco, J.Y., Rufian, J.S. et al. (2017) A cysteine-rich protein kinase associates with a membrane immune complex and the cysteine residues are required for cell death. *Plant Physiology*, 173, 771–787.
Yao, N. & Greenberg, J.T. (2006) *Arabidopsis* ACCELERATED CELL DEATH2 modulates programmed cell DEATH. *The Plant Cell*, 18, 397–411.
Zipfel, C., Robatzek, S., Navarro, L., Oakeley, E.J., Jones, J.D., Felix, G. et al. (2004) Bacterial disease resistance in *Arabidopsis* through flagellin perception. *Nature*, 428, 764–767.

SUPPORTING INFORMATION

Additional supporting information can be found online in the Supporting Information section at the end of this article.

How to cite this article: Andrade, M.d.O., da Silva, J.C., Soprano, A.S., Shimo, H.M., Leme, A.F.P. & Benedetti, C.E. (2023) Suppression of citrus canker disease mediated by flagellin perception. *Molecular Plant Pathology*, 24, 331–345. Available from: https://doi.org/10.1111/mpp.13300